Article

Cell

A Liquid-to-Solid Phase Transition of the ALS Protein FUS Accelerated by Disease Mutation

Graphical Abstract

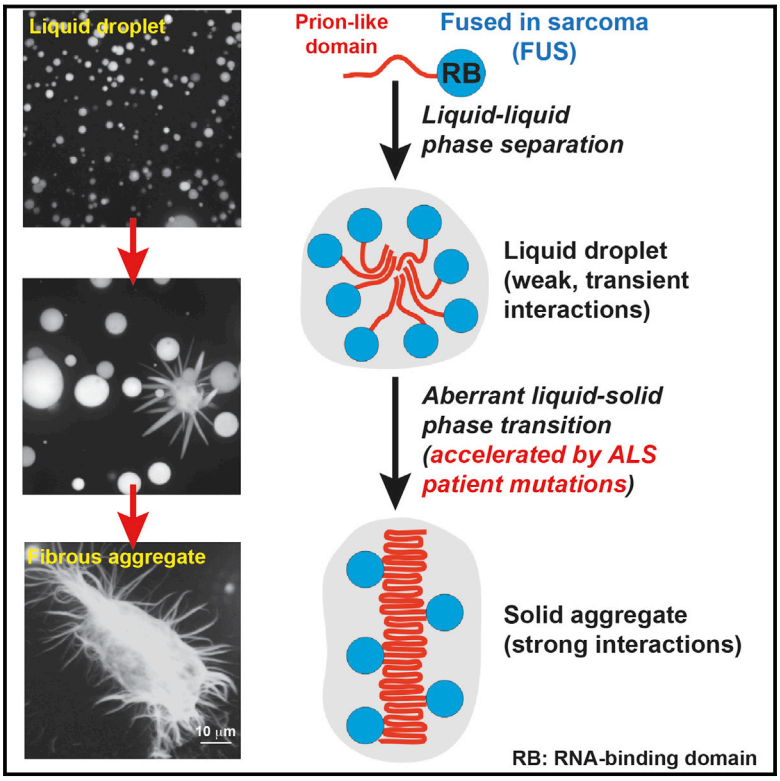

Highlights

- The ALS-associated protein FUS forms liquid compartments in vivo and in vitro
- Liquid compartment formation is dependent on the prion-like low-complexity domain
- Liquid compartments of FUS convert with time into an aberrant aggregated state
- ALS patient mutations accelerate aberrant phase transitions of FUS

Authors

Avinash Patel, Hyun O. Lee, Louise Jawerth, ..., David Drechsel, Anthony A. Hyman, Simon Alberti

Correspondence

hyman@mpi-cbg.de (A.A.H.), alberti@mpi-cbg.de (S.A.)

In Brief

The ALS-associated protein FUS assembles into a liquid-like compartment to operate in vivo, but a risk of the functionality conferred by the liquid phase is aggregation to the disease-linked solid phase. Aging diseases caused by aggregation-prone proteins may arise from a failure to maintain liquid-phase homeostasis.

Patel et al., 2015, Cell *162*, 1066–1077
August 27, 2015
http://dx.doi.org/10.1016/j.cell.2015.07.047

CellPress

Cell

Article

A Liquid-to-Solid Phase Transition of the ALS Protein FUS Accelerated by Disease Mutation

Avinash Patel,[1,6] Hyun O. Lee,[1,6] Louise Jawerth,[1,2] Shovamayee Maharana,[1] Marcus Jahnel,[1] Marco Y. Hein,[3] Stoyno Stoynov,[4] Julia Mahamid,[5] Shambaditya Saha,[1] Titus M. Franzmann,[1] Andrej Pozniakovski,[1] Ina Poser,[1] Nicola Maghelli,[1] Loic A. Royer,[1] Martin Weigert,[1] Eugene W. Myers,[1] Stephan Grill,[1] David Drechsel,[1] Anthony A. Hyman,[1,*] and Simon Alberti[1,*]

[1]Max Planck Institute of Molecular Cell Biology and Genetics, 01307 Dresden, Germany
[2]Max Planck Institute for the Physics of Complex Systems, 01187 Dresden, Germany
[3]Department of Proteomics and Signal Transduction, Max Planck Institute of Biochemistry, 82152 Martinsried, Germany
[4]Institute of Molecular Biology, Bulgarian Academy of Sciences, 21, G. Bontchev Str., Sofia 1113, Bulgaria
[5]Department of Molecular Structural Biology, Max Planck Institute of Biochemistry, 82152 Martinsried, Germany
[6]Co-first author
*Correspondence: hyman@mpi-cbg.de (A.A.H.), alberti@mpi-cbg.de (S.A.)
http://dx.doi.org/10.1016/j.cell.2015.07.047

SUMMARY

Many proteins contain disordered regions of low-sequence complexity, which cause aging-associated diseases because they are prone to aggregate. Here, we study FUS, a prion-like protein containing intrinsically disordered domains associated with the neurodegenerative disease ALS. We show that, in cells, FUS forms liquid compartments at sites of DNA damage and in the cytoplasm upon stress. We confirm this by reconstituting liquid FUS compartments in vitro. Using an in vitro "aging" experiment, we demonstrate that liquid droplets of FUS protein convert with time from a liquid to an aggregated state, and this conversion is accelerated by patient-derived mutations. We conclude that the physiological role of FUS requires forming dynamic liquid-like compartments. We propose that liquid-like compartments carry the trade-off between functionality and risk of aggregation and that aberrant phase transitions within liquid-like compartments lie at the heart of ALS and, presumably, other age-related diseases.

INTRODUCTION

Cells have a problem: How do they organize their complex biochemistry in time and space? Eukaryotic cells have addressed this problem by using functionally distinct compartments, many of which are bound by membranes. In these cases, it is easy to understand how the biochemistry is constrained in one place: the membrane prevents the diffusion of molecules in the absence of specific transport systems. However, many, if not most, cellular compartments are not membrane enclosed (Hyman and Brangwynne, 2011; Hyman et al., 2014; Li et al., 2012; Weber and Brangwynne, 2012). Examples include germ (P) granules (Brangwynne et al., 2009), processing (P/GW) bodies (Kedersha et al., 2005), stress granules (Wippich et al., 2013), nucleoli (Brangwynne et al., 2011), Cajal bodies (Strzelecka et al., 2010) and likely signaling compartments (Banjade and Rosen, 2014; Li et al., 2012). These structures are highly dynamic, and the components within them are in constant exchange with the surrounding cytoplasm or nucleoplasm. Recently, an increasing number of these non-membrane-bound compartments have been shown to behave like condensed liquid phases of the cytoplasm or nucleoplasm (Aggarwal et al., 2013; Brangwynne et al., 2009, 2011; Hubstenberger et al., 2013; Lee et al., 2013; Wippich et al., 2013). It is thought that these structures form by liquid-liquid demixing, often upon a specific triggering event.

Domains of low-sequence complexity (LC domains) have been implicated in the formation of membrane-less compartments (Decker et al., 2007; Gilks et al., 2004; Han et al., 2012; Kato et al., 2012; Malinovska et al., 2013; Toretsky and Wright, 2014). LC domains are also present in yeast prion proteins, which have the ability to interconvert into fibers rather than a liquid state (Alberti et al., 2009). Thus, proteins harboring these domains have been called "prion-like." Prion-like LC domains are particularly abundant in RNA- and DNA-binding proteins and have been conserved across evolution (Kim et al., 2013; King et al., 2012; Malinovska et al., 2013). However, mutations in prion-like proteins also cause devastating protein misfolding diseases, and these diseases are typically accompanied by the formation of solid aggregates (Gitler and Shorter, 2011; Kim et al., 2013; Li et al., 2013; Ramaswami et al., 2013). Thus, determining how prion-like proteins organize cellular compartments will not only advance our understanding of compartment formation but will also provide important insight into a diverse set of aging-associated pathologies.

One prototypical prion-like protein involved in the compartmentalization of cells is the RNA-binding protein FUS. It is enriched in the nucleus and involved in transcription, DNA repair, and RNA biogenesis (Polymenidou et al., 2012; Wang et al., 2008, 2013). Mutations in FUS are associated with amyotrophic lateral sclerosis (ALS) and rare forms of frontotemporal lobar

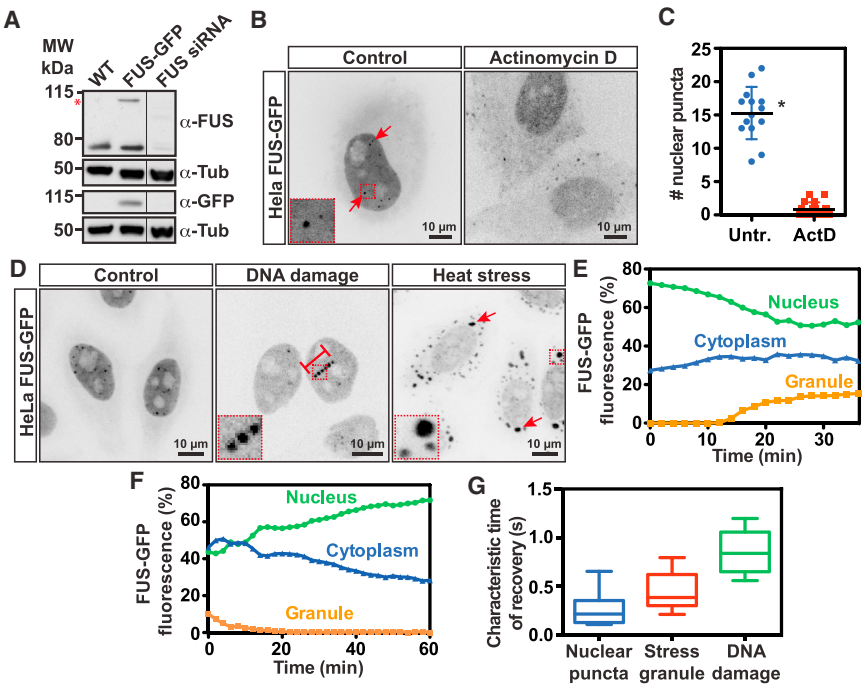

Figure 1. FUS Forms Several Dynamic Compartments In Vivo

(A) Immunoblot of Kyoto HeLa cells without a BAC transgene (WT) or with a BAC transgene for expression of FUS-GFP (FUS-GFP). FUS-GFP cells with FUS small interfering RNA (siRNA) treatment (FUS siRNA). The expected molecular weight (MW) of endogenous FUS is 75 kDa. The asterisk marks transgenic FUS-GFP. The FUS-GFP expression level (estimated by band intensity) is approximately 60% of the endogenous FUS. The total amount of FUS expressed in FUS-GFP cells (endogenous plus FUS-GFP) is about 1.75-fold higher than the FUS expression in wild-type cells. α-Tub, α-tubulin.

(B) Inverted black and white images of FUS-GFP-expressing cells in control or actinomycin-D-treated conditions (nuclear puncta are magnified in the inset).

(C) Quantification of the average number of nuclear puncta in untreated (Untr.) and actinomycin-D (ActD)-treated conditions (n = at least 10 per condition). Error bars represent SD. *p < 0.00001.

(D) FUS-GFP-expressing cells in control, DNA-damage, and heat-stress conditions. Sites of strong FUS-GFP localization are shown by dark puncta at the irradiation-induced DNA damage sites (marked with red lines) and stress granules (marked with red arrows). The insets show approximately 13-fold magnifications of the FUS compartments.

(E) FUS-GFP fluorescence in the nucleus, cytoplasm, and stress granules (Granule) were measured after the induction of stress (time point 0) by time-lapse imaging. The representative graph reports the fluorescence intensity in each compartment.

(F) FUS-GFP fluorescence in the nucleus, cytoplasm, and stress granules (Granule) were measured after the release of stress (time point 0) by time-lapse imaging.

(G) Recovery half-times (Characteristic time of recovery) of FUS-GFP fluorescence after photobleaching in the nuclear puncta, stress granules, and DNA damage sites (n = 10 per condition). For nuclear puncta versus stress granule, p = 0.1016; for nuclear puncta versus DNA damage sites, p = 0.0004; for stress granule versus DNA damage site, p = 0.0089. The line within the boxplot represents the median, and the outer edges of the box are the 25th and 75th percentiles. The whiskers extend to the minimum and maximum values.

See also Movie S1.

degeneration (FTLD) (Deng et al., 2014; Woulfe et al., 2010). Recent reports show that the prion-like LC domains of FUS can polymerize into fibrous amyloid-like assemblies in a cell-free system (Han et al., 2012; Kato et al., 2012; Kwon et al., 2013, 2014). Once assembled, these structures exhibit the macroscopic behavior of hydrogels. However, it has been difficult to understand the relationship between amyloid-like hydrogels that form in vitro and the in vivo function of the protein, because there has been little work on the dynamics of FUS in living cells and the relationship between this dynamic behavior and the onset of disease.

Here, we show that both in vivo and at physiological concentrations in vitro FUS forms liquid-like droplets. We further demonstrate that the liquid-like state can convert into a solid state and that this conversion is exacerbated by disease-associated mutations in the prion-like domain. Our findings suggest that aberrant phase transitions may be at the heart of many neurodegenerative diseases.

RESULTS

The Prion-like Protein FUS Assembles into Various Dynamic Compartments In Vivo

Previous reports have implicated FUS in the formation of stress-inducible compartments, such as DNA damage sites and stress granules (Li et al., 2013; Mastrocola et al., 2013; Rulten et al., 2014; Wang et al., 2013). These studies often used transient transfection protocols and overexpression plasmids to study the subcellular localization of FUS. We used an approach based on BAC (bacterial artificial chromosome) transgeneOmics (Poser et al., 2008). BACs have the advantage that they allow the expression of transgenes from their native genomic environment, including most, if not all, regulatory elements. First, we generated a BAC transgene for the expression of GFP-tagged FUS and introduced it into HeLa and embryonic stem (ES) cells to generate stable cell lines (Figure 1A). Next, we used mass spectrometry to determine the physiological concentration of FUS in HeLa cells (Figure S1A). We found that the concentration is around 2 μM, with a technical precision between replicates of 2.24 ± 0.7 μM and an estimated accuracy of 2- to 3-fold (Wiśniewski et al., 2014). This makes FUS one of the top 5% of proteins in terms of protein abundance. Because FUS is 2- to 4-fold enriched in the nucleus under normal conditions (Figure S1B), the local concentration in the nucleus may be between 4 and 8 μM.

Using FUS-GFP HeLa cells, we found that, in unstressed cells, FUS predominately localized to the nucleus (Figure 1B), in agreement with previous reports. We also noticed that FUS formed small foci in the nucleoplasm (Figure 1B). A similar distribution was observed in mouse ES cells (Figure S1C). Cells treated

with actinomycin D, a potent inhibitor of RNA polymerase II, showed no nuclear assemblies (Figures 1B and 1C), confirming previous observations that FUS is involved in transcription regulation and splicing (Kwon et al., 2013; Schwartz et al., 2012; Yang et al., 2014). This suggests that, under normal conditions, FUS assembles into compartments that may be associated with transcription or splicing.

FUS has also previously been implicated in DNA repair (Rulten et al., 2014; Wang et al., 2013). Indeed, we found that FUS accumulated at DNA lesions within a second of laser-mediated irradiation (Figures 1D, S1C, and S1D; Movie S1). Next, we exposed the FUS cell line to heat stress to induce previously reported stress-associated compartments in the cytoplasm (Bosco et al., 2010; Li et al., 2013). Indeed, FUS accumulated in the cytoplasm in heat-stressed cells and coalesced into stress granules (Figures 1D and S1E; Movie S1). Formation and dissolution of these stress granules was coupled to changes in cytoplasmic and nuclear FUS levels (Figures 1E, 1F, and S1E; Movie S1), suggesting that the coalescence of these compartments occurs over a certain concentration of soluble components. To further investigate the dynamics of FUS protein in these compartments, we photobleached FUS-containing cellular structures and followed the recovery of the fluorescence over time. Indeed, for all three structures examined, we observed a rapid exchange between assembled and soluble FUS, with a half-time of recovery ranging from hundreds of milliseconds to 1 s (Figures 1G and S1F).

Our data so far support previous work showing that FUS localizes to multiple different compartments, depending on the type of stress the cell is experiencing. Our data further suggest that these compartments are extremely dynamic. In the nucleus, FUS localizes to active sites of transcription and rapidly assembles on sites of DNA damage. Upon heat shock, FUS shuttles out to the cytoplasm, where it forms a compartment in a concentration-dependent manner. In all these compartments, FUS turns over within hundreds of milliseconds to around 1 s.

FUS Compartments Have Liquid Properties In Vivo

The dynamic nature of FUS compartments is reminiscent of other RNA protein compartments such as P granules and nucleoli, which form by liquid-liquid demixing in the cytoplasm or nucleoplasm. Three characteristics define a liquid-like compartment. First, the components should undergo rapid internal rearrangement. Second, the compartments should be roughly spherical due to surface tension. Third, two droplets should fuse and relax into one droplet. Therefore, we tested whether FUS compartments have these liquid-like characteristics.

The constant mixing of components within a liquid can be tested by a technique known as "half-bleach" (Brangwynne et al., 2009; Hyman et al., 2014). In this method, roughly half a structure is bleached, and then the distribution of the fluorescence within the photomanipulated structure is determined over time (see Experimental Procedures for details). The spatiotemporal analysis of such half-bleach events showed that FUS was redistributed rapidly within stress granules and nuclear FUS assemblies, from the unbleached area to the bleached area (Figures 2A and 2B; Figure S2A; Movie S2). Thus, we conclude that FUS molecules can diffuse freely in stress granules and nuclear assemblies, in agreement with a liquid material state.

To investigate the shape of stress-induced FUS structures, we observed FUS-GFP-expressing cells with a digital scanned light-sheet microscope (DSLM) with structured illumination, which allows improved 3D imaging of dynamic subcellular objects (Gao et al., 2014). Using this imaging technology, we found that FUS granules are spherical (Figure 2C). The calculated sphericity was close to that of a perfect sphere for both heat-induced and arsenate-induced cytoplasmic FUS granules (Figure 2D). We cannot measure the sphericity of the nuclear structures because they are too small. We then used DSLM microscopy to perform a time-resolved analysis of individual FUS granules in the cytoplasm. We found that FUS granules underwent frequent fusion events and, as soon as they interacted, rapidly relaxed into a spherical shape (Figures 2E and S2B; Movie S2). The relaxation time of these granules was on the order of a few minutes (Figure 2F). Using the relaxation time and the FRAP (fluorescence recovery after photobleaching) times, we approximated viscosity values, as previously described (Brangwynne et al., 2009). We estimate viscosities around 10- to 100-fold of water (10–100 mPa•s). We were unable to see fusion events for nuclear FUS compartments, presumably because they are fixed in place on the DNA.

Therefore, FUS assemblies have all the hallmarks of a liquid state: they turn over quickly; are spherical; and when they fuse, they relax into one spherical assembly (Hyman et al., 2014). Taken together, these experiments show that FUS assemblies are liquid droplets, which probably form by liquid-liquid demixing in the cytoplasm or nucleoplasm.

Recombinant FUS Phase Separates into Dynamic Liquid Droplets In Vitro

Our data so far indicate that FUS is a component of liquid-like compartments in vivo that form by demixing from the cytoplasm. To investigate whether FUS is able to phase separate on its own, we studied the behavior of recombinant GFP-tagged FUS expressed in insect cells (see Experimental Procedures for details) (Figures 3A and 3B; Figures S3A and S3B). For these experiments, we chose a FUS-GFP concentration of 10 μM, which is slightly higher than the measured physiological concentration (Figure S1A) but easier to work with in our imaging-based assays. At this concentration, we found that FUS was diffusely distributed (Figure 3C). At a concentration of 500 μM, about 100-fold higher than the physiological concentration, FUS formed a gel-like state (Figure 3C; Movie S3), as previously reported (Kato et al., 2012).

Because of the discrepancy with our in vivo data, which shows that FUS coalesces into liquid compartments in living cells, we looked for conditions that promote FUS assembly into compartments at physiological concentrations. A 10% solution of either dextran or polyethylene glycol (PEG) induced assembly of FUS into round micrometer-sized structures (Figures 3C and S3C–S3G). To characterize whether these FUS assemblies have liquid-like properties, we performed a series of biophysical experiments. First, we investigated whether FUS molecules can freely move around within the droplets. Indeed, the FUS signal rapidly rearranged from the unbleached region to the bleached region of a half-bleached droplet (Figures 3D–3F and S3H; Movie S4), consistent with a high internal mobility. The ability of a droplet to deform or of two droplets to fuse also helps distinguish

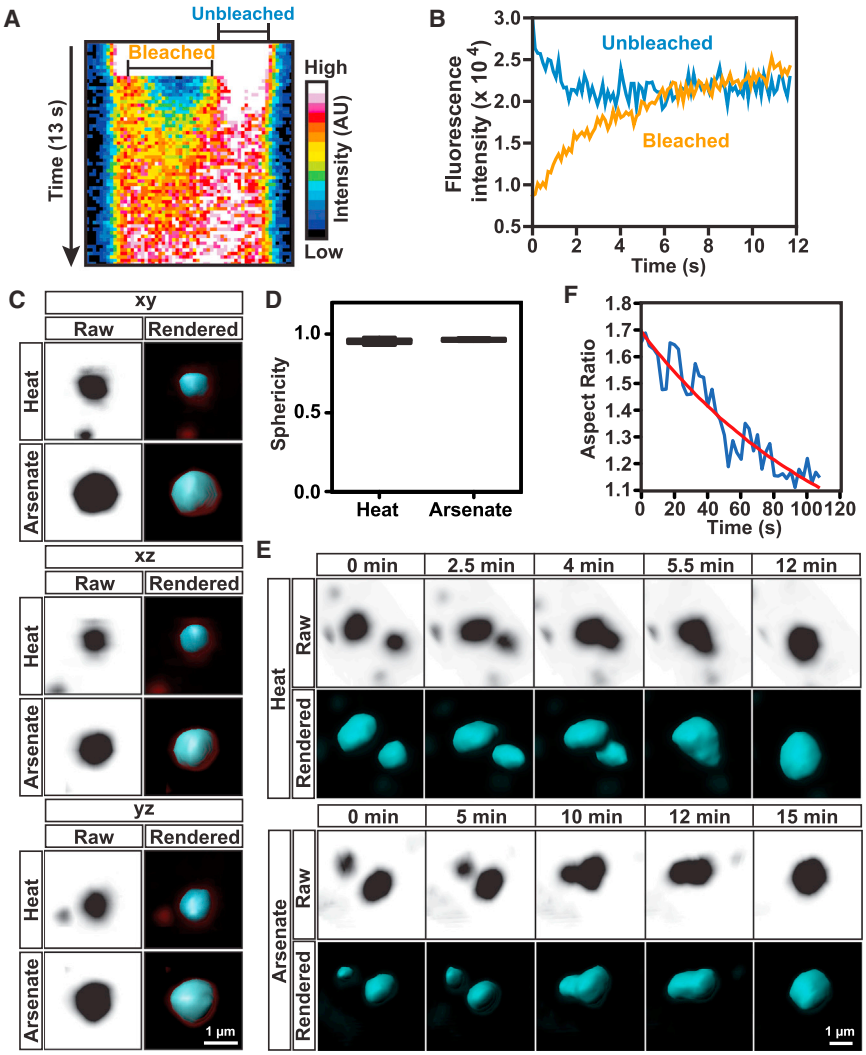

Figure 2. FUS Compartments Have Liquid-like Properties In Vivo

(A) Representative heatmap kymograph showing fluorescence intensity within one half-bleached FUS-GFP stress granule over time. AU, arbitrary units.

(B) Internal rearrangement of fluorescent FUS-GFP molecules within a half-bleached FUS-GFP stress granule in (A) is shown by quantification of fluorescence in bleached (orange line) versus unbleached regions (blue lines) over time. Intensity changes in a bleached or an unbleached pixel region over time was plotted.

(C) Raw and rendered 3D shapes of a stress granule in heat- or arsenate-stressed living cell. The panels show the xy, xz, and yz planes, respectively.

(D) A plot showing the sphericity values of heat- or arsenate-induced stress granules (n = 10 per condition). A value of 1 represents a sphere. Error bars represent SD. p = 0.5445.

(E) Raw and rendered montages of FUS-GFP stress granule fusion events in heat- and arsenate-induced stress conditions.

(F) The shape changes of an FUS-GFP droplet over the time course of a fusion event measured as aspect ratio (ratio between the long axis and the short axis of a stress granule over time with an exponential fit). As fused granules relax to a spherical shape, the aspect ratio reaches 1.

See also Movie S2.

liquids from solid gels (Hyman et al., 2014). Therefore, we next asked whether FUS droplets are deformable by shear force. Indeed, under such conditions, FUS droplets changed their shape, as would be expected for a dynamic liquid with no memory of its previous state (Figure 3G; Movie S4). Furthermore, we found that when two FUS droplets touched each other, they rapidly fused and relaxed into one larger droplet within seconds (Figures 3H and S3I; Movie S4). Such rapid relaxation times are expected for liquid droplets with low viscosity.

Previous studies had identified the N-terminal prion-like domain as critical for the formation of hydrogels (Kato et al., 2012). Therefore, we generated a deletion mutant of FUS lacking this N-terminal domain (FUSΔLC) and purified it from insect cells using the same protocol as for wild-type FUS. When we mixed 10 μM of wild-type or FUSΔLC protein with 10% dextran, only wild-type protein formed droplets, whereas truncated FUS remained diffuse (Figure S3J). This indicates that the prion-like domain is essential for forming liquid droplets, presumably because of its sticky nature and ability to undergo many weak interactions.

Therefore, FUS structures have all the hallmarks of liquid droplets both in vivo and in vitro: they are spheres, they fuse, they deform under shear stress, and they rearrange their contents within seconds. This indicates that under physiological conditions, FUS does not assemble into solid-like aggregates or gels but rather forms dynamic droplets that exhibit all the properties of a true liquid. It further confirms that FUS has an intrinsic ability to phase separate and form liquid droplets, suggesting that FUS may play a central role in forming liquid compartments at sites of DNA damage and during stress.

Multivalent PAR Chains Nucleate FUS Droplets In Vivo and In Vitro

Previous studies identified a poly(ADP) ribose (PAR)-binding domain in the C-terminal region of FUS and showed that FUS is rapidly recruited to DNA damage sites in a PAR-dependent manner (Mastrocola et al., 2013). Indeed, we found that PAR polymerase 1 (PARP1) arrives within seconds of DNA damage, and FUS was detectable immediately after arrival of PARP1 (Figure 4A). To investigate whether PAR is required for FUS accumulation, we interfered with PAR formation by adding an inhibitor of PARP1/2 to cells shortly before laser-mediated irradiation (Rulten et al., 2014). Indeed, inhibition of PARP1/2 prevented the recruitment of FUS (Figures 4B and 4C). Conversely, inhibition of a PAR-degrading enzyme (PARG) prolonged the presence of

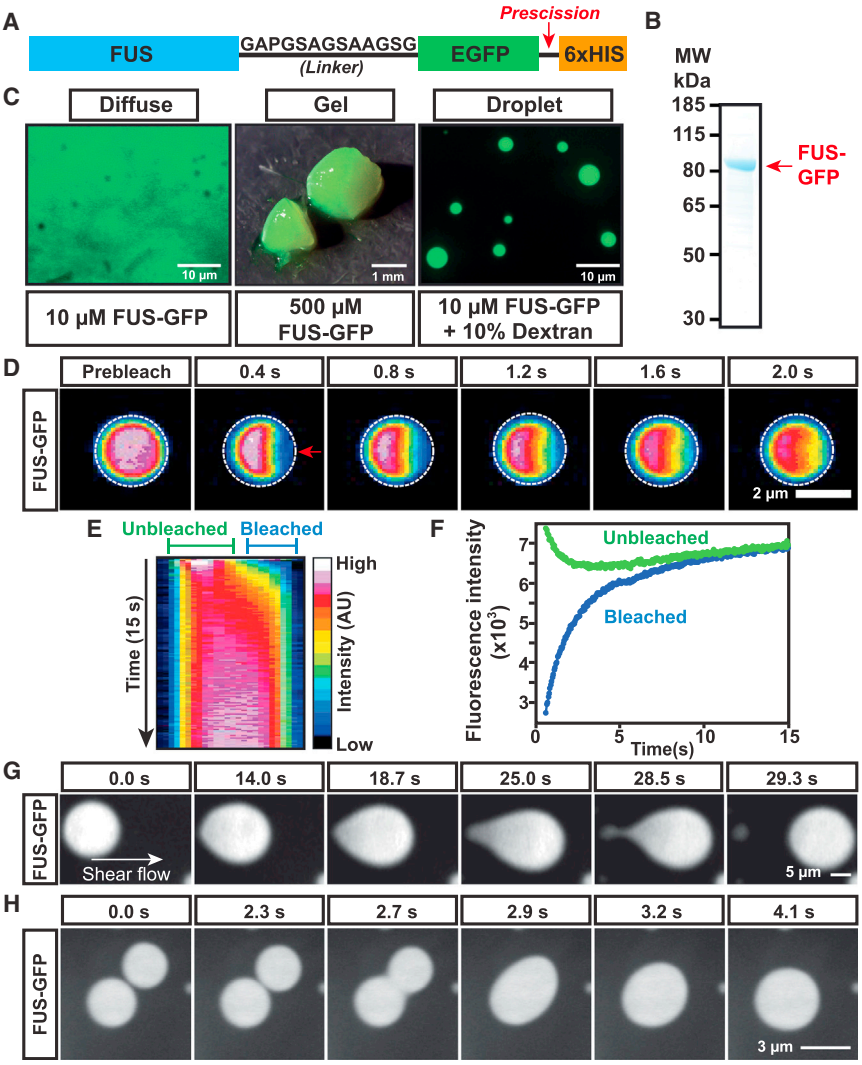

Figure 3. Reconstituted FUS Compartments Have Liquid-like Properties

(A) Recombinant human FUS was tagged with GFP at the C terminus, separated by a 13-amino-acid linker. The protein was purified from insect cells, and the His tag was cleaved off using Prescission Protease.

(B) Coomassie-stained SDS-PAGE gel of purified FUS-GFP (~82 kDa). MW, molecular weight.

(C) Purified FUS-GFP investigated by fluorescence microscopy. Diffuse: 10 µM FUS-GFP. Gel: 500 µM FUS-GFP. Droplet: 10 µM FUS-GFP in the presence of a molecular crowder (10% dextran). Also see corresponding Movie S3 for FUS-GFP gel.

(D) Recovery of fluorescence intensity of an in-vitro-formed FUS-GFP droplet after half-bleach. The site of bleach is marked by a red arrow.

(E) Representative heatmap kymograph showing fluorescence intensity within a half-bleached in vitro FUS-GFP droplet over time shown in (D). AU, arbitrary units.

(F) Internal rearrangement of fluorescent FUS-GFP molecules within a half-bleached FUS-GFP droplet in (D and E) is shown by the quantification of the fluorescence intensity in the bleached (blue line) and unbleached (green line) regions of the droplet. Intensity changes in a bleached or an unbleached pixel region over time was plotted. Please note that the continuous upward slope of both the bleached and unbleached region is due to exchange of molecules from solution.

(G) Montage of an FUS-GFP droplet deforming under shear flow.

(H) Montage of two FUS-GFP droplets fusing under shear flow.

See also Movies S3 and S4.

FUS at DNA lesions (Figures 4B and 4D). This suggests that PAR polymers are required for the recruitment as well as the prolonged presence of FUS in DNA damage-associated compartments. To study whether PAR affects FUS droplet formation in vitro, we first adjusted the FUS concentration in our cell-free assay to 0.4 µM and lowered the concentration of dextran. At this concentration, we observed no spontaneously formed FUS droplets. However, when purified PAR was added, FUS droplet formation was strongly enhanced (Figures S4A–S4C). In summary, these data provide evidence for the intrinsic ability of multivalent PAR chains to nucleate the formation of FUS droplets. Therefore, we conclude that local PAR synthesis and the cooperative PAR-binding activity of FUS are required to drive the formation of a non-membrane-bound compartment for DNA repair.

Droplets Formed from Mutant FUS Have Different Biophysical Properties

FUS can form pathological protein aggregates, and specific mutations in FUS have been identified in patients suffering from neurodegenerative diseases (Deng et al., 2014). Previous studies have shown that a patient-derived mutation in the prion-like domain of FUS (G156E) has an increased tendency to form aggregates (Nomura et al., 2014). To investigate the link between the compartment-forming abilities of FUS and disease, we expressed G156E FUS-GFP in insect cells and purified the protein using the same protocol as used previously for wild-type FUS (Figures 5A and 5B). When 10 µM wild-type FUS and G156E FUS were incubated in 500 mM salt, only diffuse fluorescence was seen over many hours (Figure S5A). Upon dilution of G156E FUS to a concentration of 10 µM in the presence of dextran, we found that it formed liquid-like structures, similar to those observed for wild-type FUS. We were also unable to observe any obvious differences in the properties of G156E and wild-type droplets (data not shown). In addition, we expressed G156E FUS-GFP from a BAC transgene in HeLa cells, but we could not detect any obvious differences in FUS compartments formed in wild-type cells (data not shown).

Next, we set up an "aging" experiment in which we added dextran to FUS solutions and monitored the behavior of the droplets with time. Using an optical tweezer, we first showed

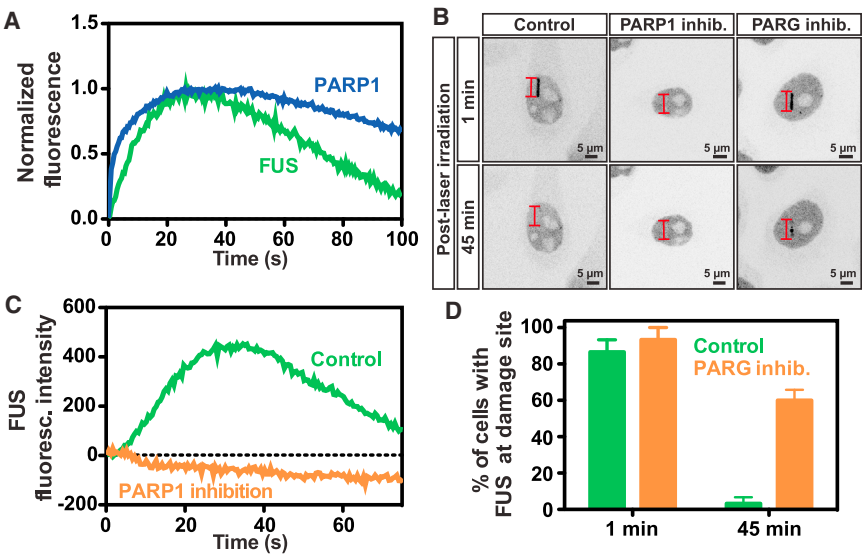

Figure 4. Poly(ADP) Ribose Formation Nucleates FUS Compartments In Vitro and In Vivo

(A) HeLa cells expressing FUS-mCherry and PARP1-GFP are imaged after DNA damage induction by laser micro-irradiation. Normalized fluorescence intensity of FUS-mCherry (green) or PARP1-GFP (blue) at DNA damage sites is plotted over time after DNA damage induction.

(B) FUS-GFP-expressing cells at 1 min and 45 min after DNA damage induction by laser micro-irradiation in control, PARP1-, or PARG-inhibitor (inhib.)-treated conditions. Sites of laser micro-irradiation are shown by red lines. Dark puncta are sites of strong FUS-GFP concentration.

(C) Representative graph showing the FUS-GFP fluorescence (fluoresc.) intensity in control (green) and PARP-inhibitor (orange) conditions over time after DNA damage induction.

(D) Percentage of cells with FUS-GFP at damage sites in 1 or 45 min after DNA damage in control and PARG-inhibitor-treated conditions (n = 10 per condition). Error bars represent SD. The p value at 1 min = 0.5185; the p value at 45 min = 0.0011.

that one FUS droplet held by one laser beam can fuse with several other droplets (Movie S5). To quantify this behavior, we used two laser beams to control fusion events (Figure 5C; Movie S6). The results of a typical experiment are shown in Figure 5D. Between 0 and 2 hr after droplet formation, wild-type FUS droplets fused very quickly, often within hundreds of milliseconds (Movie S6). Similar behavior was seen for G156E FUS. However, the relaxation time of G156E FUS was significantly longer than for wild-type FUS (Figure 5E), and the spread of values became much broader, with some droplets taking as long as 15 s to fuse. More strikingly, as the droplets aged in a test tube, we noticed that an increasing fraction of the G156E FUS droplets no longer fused (Figure 5F; Movie S6) so that, after 8 hr, we could detect no fusion events for G156E FUS, while 81% of the wild-type FUS droplets still fused. By 12 hr, wild-type droplets also stopped fusing. This indicates that there is indeed a change in the biophysical properties of FUS droplets with time. It further suggests that the properties of the G156E FUS droplets are changing more quickly than those of the wild-type FUS droplets. This is consistent with the observation that G156E has a higher propensity to aggregate as observed by Nomura et al. (2014). Concomitant with the decline in fusion ability, we also noticed fibrous structures arising in the G156E FUS droplets (Figure S5B; Movie S7). Therefore, we conclude that FUS droplets age and undergo drastic changes in their biophysical properties and morphology.

Patient-Derived Mutations Promote a Conversion of FUS from a Droplet to a Fiber State

Next, we investigated the aging morphology of FUS droplets by fluorescence microscopy. Figure 6A shows a typical experiment. For wild-type FUS, the droplets increased in size with time so that, by 8 hr, large droplets were observed in all fields. For G156E FUS, the droplets also increased in size. However, by 8 hr, hardly any G156E droplets remained. Rather, only fibrous structures could be seen (Figure 6A). For wild-type FUS, mainly droplets were seen by 8 hr, although some fibers were now detectable as well. By 12 hr, most of the wild-type FUS protein had converted into fibers, but a few droplets could still be observed. Next, we investigated another patient-derived mutant of FUS with a mutation adjacent to the prion-like domain (R244C) and found that R244C also accelerated the conversion of FUS droplets to a fibrous state (Figure S6A).

Therefore, we can conclude that, with time, a solution of FUS containing liquid droplets will convert into fibrous structures. Although wild-type and mutant FUS convert from droplets to fibers, the mutant consistently converts more quickly than the wild-type. When we looked more carefully at the time points containing aggregates, we saw that some of the droplets had short fibers (Figure 6A), while others had much longer fibers emanating from them. We call these structures with small fibers "sea urchins," because they are reminiscent of similarly named transition structures seen in crystallization studies (Vekilov, 2004), and longer fibers "starbursts" (Figure 6B; Movie S7). Time-lapse imaging of the sea urchins revealed that the fibers protruding from the surface continuously grew until the structure resembled that of a commonly observed starburst (Movie S7). One intriguing possibility is that this structure is the transition structure of a droplet converting into fibers. Such a process is consistent with the droplets acting as centers of fiber nucleation and growth.

To quantify the biophysical properties of the FUS fibers, we performed photobleaching experiments on structures from wild-type and G156E FUS. At t (time) = 0, both wild-type and G156E droplets recovered quickly after photobleaching (Figure 6C). However, by t = 8 hr, the G156E structures no longer recovered, suggesting that they interconverted from a liquid to an aggregated state. Even within one fibrous structure, the fibers projecting out turned over more slowly than the body (Figure S6B). This shows that, over time, a population of FUS protein converts from a liquid to a solid state. We confirmed this by performing cryoelectron microscopy (cryo-EM) studies of the droplet and fiber state. We found that FUS droplets were

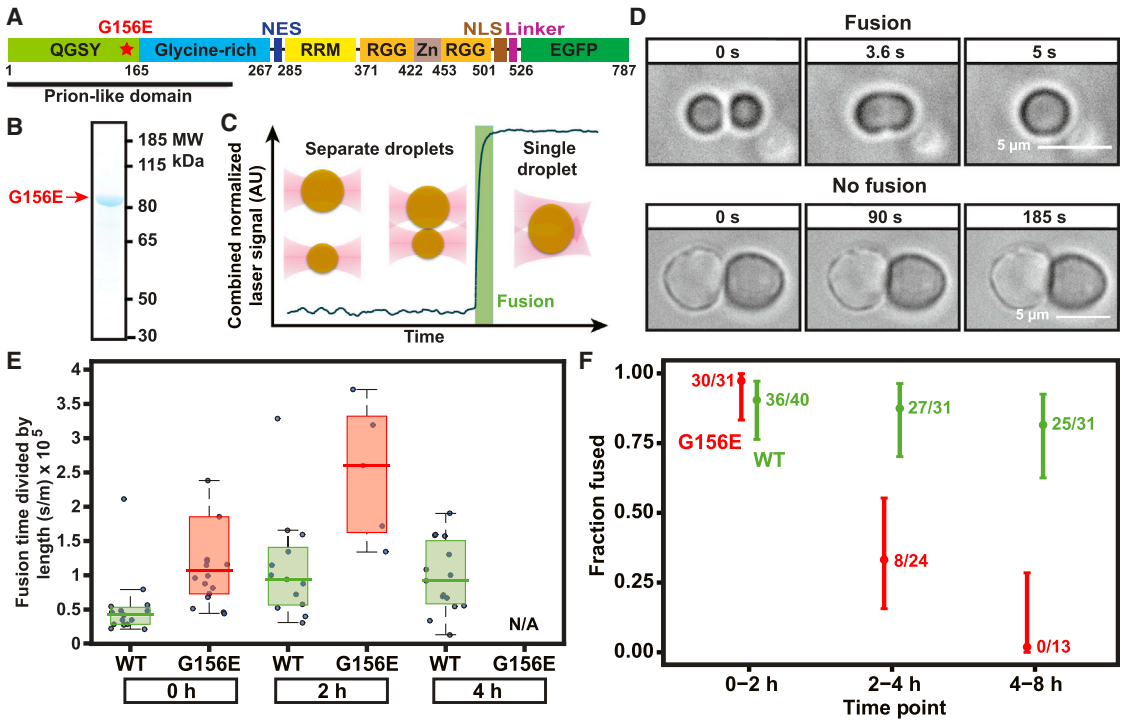

Figure 5. The Physical Properties of FUS Droplets Change with Time and Are Accelerated by a Patient-Derived Mutation in the Prion-like Domain

(A) Recombinant human FUS with a single ALS-associated mutation (G156E, ★) in the prion-like domain was expressed and purified from insect cells.

(B) Coomassie-stained SDS-PAGE gel of purified G156E FUS-GFP (~82 kDa). MW, molecular weight.

(C) Diagram illustrating the method to control in vitro fusion experiments using two optical traps demonstrated by the signal of two FUS droplets. The green bar indicates the time of a fusion event, which can be inferred from the increase in the combined normalized laser signal. AU, arbitrary units.

(D) Representative montages of "fusion" and "no-fusion" events in the optical trap experiments.

(E) A boxplot of fusion times of wild-type (WT) and G156E FUS-GFP droplet pairs scaled by the mean drop size at different time points using optical trap. The line within the boxplot represents the median and the outer edges of the box are the 25th and 75th percentiles. The whiskers extend to the most extreme points not considered outliers. Outliers are calculated as the points that are smaller than $q_1 - 1.5(q_3 - q_1)$ and larger than $q_3 - 1.5(q_3 + q_1)$, where q_1 and q_3 are the 25th percentile and 75th percentile, respectively. N/A indicates that fusion times could not be determined because fusion events were no longer detectable. s, seconds; h, hour.

(F) Fraction of wild-type (WT) and G156E FUS-GFP droplet pairs showing fusion at different time points in vitro using an optical trap. Error bars represent binomial confidence intervals. h, hours.

See also Movie S6.

amorphous and lacked ordered structures (Figure S6C). The fiber state of FUS, instead, was characterized by many fibrillar assemblies with a diameter of around 9 nm, and many of these fibrils were laterally aligned (Figure S6C). These structures are reminiscent of the amyloid-like aggregates identified in previous work (Kato et al., 2012). Thus, we conclude that the liquid droplet state is metastable and transitions into a thermodynamically more stable aggregated state with time.

Many ALS-associated mutations map to the C-terminal nuclear localization sequence (NLS) of FUS. Mutations in the NLS increase the cytosolic fraction of FUS (Kwiatkowski et al., 2009; Vance et al., 2009). We confirmed this result by making a BAC cell line containing a deletion of the NLS (Figure S6D). Because phase transitions are extremely sensitive to protein concentration, we hypothesized that these NLS mutations could accelerate the conversion of FUS to a fibrous state by increasing the concentration of FUS in the cytoplasm. Indeed, we found that increasing concentrations of FUS had a higher propensity to convert from a droplet to a fibrous state (Figures S6E and S6F). Therefore, we conclude that the aggregation of FUS is concentration dependent and that ALS-associated mutations in FUS may promote the formation of aggregates as seen in patient cells by accelerating the conversion from a liquid droplet to a fibrous state.

DISCUSSION

In this paper, we show that, both in vivo and at physiological protein concentrations in vitro, the prion-like protein FUS forms liquid compartments. The evidence for this is 3-fold. First, the individual FUS molecules rapidly rearrange within the compartment. Second, the compartments formed by FUS are spherical. Finally, two FUS compartments can fuse and relax into one sphere. FUS rapidly shuttles between liquid compartments in the nucleus and the cytoplasm depending on the type of stress. Importantly, we show that, with time, a population of FUS

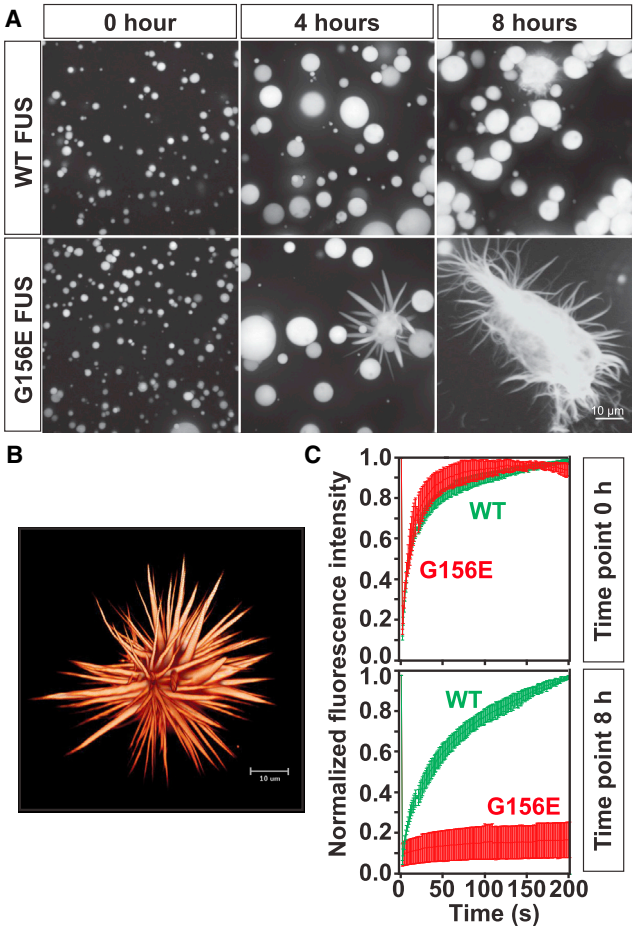

Figure 6. FUS Converts from a Liquid Droplet to Fibrous Aggregates

(A) Representative images of the morphological changes in in vitro droplets of wild-type (WT) or G156E FUS-GFP during an "aging" experiment over 8 hr.

(B) 3D rendered morphology of a G156E FUS-GFP "starburst."

(C) Recovery of fluorescence after photobleaching of wild-type (WT) FUS-GFP or G156E FUS-GFP assemblies at time points 0 and 8 hr (h). Error bars represent SD over seven independent measurements.

See also Movie S7.

droplets converts from a liquid state to an aggregated state, which is reminiscent of the pathological state seen in ALS patients with mutations in the FUS protein. This conversion from liquid to solid is accelerated either by mutations in the prion-like domain that induce the early onset of ALS or by raising the protein concentration, which mimics mutations in the NLS. Therefore, our data suggest that aberrant phase transitions may be at the heart of ALS and potentially other related diseases.

FUS compartments are a member of an expanding set of RNA-protein compartments, such as P granules and nucleoli, which probably form by liquid-liquid demixing from cytoplasm. Demixing, or phase separation, is a powerful way to locally and rapidly form compartments when needed. Indeed, FUS moves to sites of DNA damage within seconds of a triggering event, presumably forming a compartment that recruits myriad additional factors required for DNA damage repair (Dutertre et al., 2014; Lukas et al., 2011). The liquid-like nature of the compartment means that DNA repair enzymes could diffuse rapidly within the compartment, while the phase boundary would maintain a high local concentration of these enzymes and provides identity to the compartment (Hyman and Brangwynne, 2011; Hyman et al., 2014; Weber and Brangwynne, 2012).

Solid aggregates of FUS protein are commonly seen in ALS patients. However, our results clearly show that, under physiological conditions, FUS forms a liquid. Therefore, the onset of ALS must involve, in some way, a transformation from a liquid to an aggregated state. One explanation for this transformation is that the raised concentration of FUS in liquid compartments triggers aggregation. In fact, many experiments in vivo and in vitro have shown that increasing the concentration of FUS converts the protein into an aggregated state (Shelkovnikova et al., 2014; Sun et al., 2011). This is presumably the mechanism underlying patient mutations in the NLS of FUS, which also leads to an increased cytoplasmic concentration (Kwiatkowski et al., 2009; Vance et al., 2009). Indeed, we have shown that, in vitro, the conversion from liquid to a solid-like state is concentration dependent (Figure S6F). The liquid-to-solid phase transition that we observe in vitro is reminiscent of the process of protein crystallization, where formation of a metastable liquid phase often precedes the formation of crystals. Although the chemistry and physics of protein crystallization is not fully understood, it is thought that the higher density of proteins in the liquid phase triggers nucleation of the crystal (Dumetz et al., 2008; Galkin and Vekilov, 2000; Lomakin et al., 2003; Vekilov, 2010). An alternative idea is that the orientation and the altered dynamics of the molecules at the phase boundary promote crystal formation (Vekilov, 2004).

The droplets with fibers protruding from them are remarkably similar to the transition states in protein crystallization studies. For instance, when lysozyme or hemoglobin is crystalized, intermediate liquid droplets can be seen with small fibers emanating from them (Galkin et al., 2002; Galkin and Vekilov, 2000; Vekilov, 2004). These states are also reminiscent of previously reported states that precede the formation of amyloid in in vitro aggregation reactions of the yeast prion Sup35 (Serio et al., 2000). An alternative idea would be that there are two competing reactions in a test tube: liquid compartment formation and fibrous aggregation. Compartment formation is much quicker, but the soluble protein could slowly aggregate in the background, thus depleting the pool of monomeric FUS and leading to disassembly of the FUS droplets over time. We think this idea is less compelling, because we observe a decrease in droplet fusion with time, a change in droplet morphology, and also the droplets increase in size during incubation (compare panels 0 hr and 4 hr in Figure 6A). However, most likely, both conversion of liquid droplets into fibers structures and a fibrous aggregation reaction in the solution are taking place at the same time.

One problem is that we still do not know how pathological aggregates arise in living cells. Do they form in liquid compartments, or do they form in the bulk cytoplasm or nucleoplasm? We speculate that the liquid-solid transformation of FUS initially takes place in subcellular compartments but that later stages of the disease are characterized by aggregation reactions occurring in a compartment-independent manner. This is because

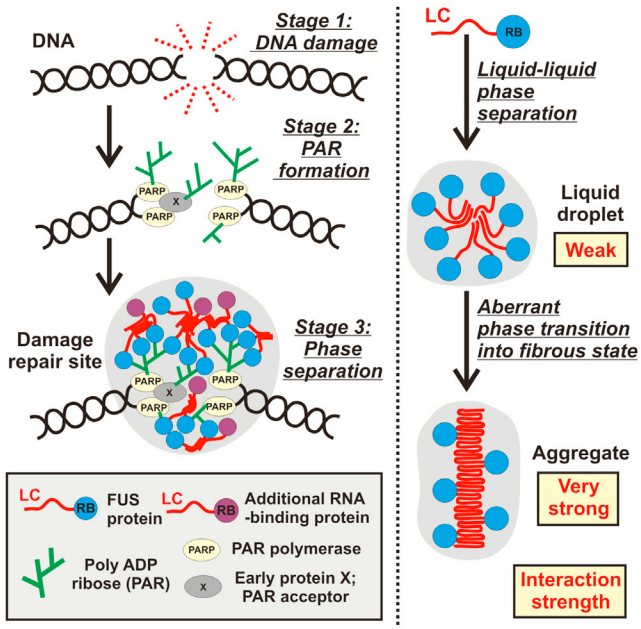

Figure 7. Diagram Illustrating the Molecular Mechanisms Underlying the Formation of FUS Compartments and Their Conversion into an Aggregated State

Left: FUS compartment formation upon DNA damage is driven by PAR polymerase and local PAR formation. PAR polymerase and other proteins (X) are modified with PAR chains in the process. PAR formation leads to FUS recruitment and initiates phase separation and compartment formation through LC domain interactions. Other proteins, such as EWS and TAF15 are likely recruited, thus forming a compartment for DNA damage repair. Right: FUS compartments form through phase separation from a concentrated solution of FUS, a reaction probably driven by weak interactions between prion-like LC domains. Liquid FUS droplets convert with time into an aggregated state, which presumably is associated with disease. LC domains are indicated in red; RB, RNA- and PAR-binding domains, indicated in blue.

amyloid-like aggregates are highly infectious, and once they have formed, they can seed further aggregation reactions in the same or in neighboring cells (Jucker and Walker, 2013).

We were surprised to see that two distinct point mutations induced such a strong effect in vitro, whereas the disease would only manifest in a living organism after many years. However, in vivo, there will be many factors that are working against aberrant conformations, such as molecular chaperones and ATP-consuming degradation machines. As these control mechanisms weaken with age (Taylor and Dillin, 2011), there presumably is a decline in the ability of a cell to counteract the formation of aberrant conformational states in compartment-forming proteins. Indeed, in vitro, we see both the wild-type and mutant FUS droplets changing biophysical properties, although the mutant changes more quickly than the wild-type protein. Therefore, it may be difficult to recapitulate the mutant state of the protein in living cells, because disease formation is a gradual process and young cells have very active quality control machinery in place. Indeed, our preliminary results suggest that when G156E FUS is expressed from its own promoter in HeLa cells, it has similar dynamics as wild-type FUS. Future work in differentiated neuronal systems will be required to identify the specific mechanisms that fail on a pathway to disease.

Recent work has shown that at high concentrations, the prion-like LC domain of FUS forms amyloid-like fibers and that this leads to hydrogel formation in a test tube (Kato et al., 2012). These experiments were operating at ~100 times the physiological cellular concentration and, therefore, are unlikely to represent the physiological state of the protein, which we think is a liquid state. However, it seems likely that these amyloid structures are similar or identical to the fibrous aggregates that we see in our in vitro aging experiments. Therefore, taken together, we can propose the following model as to how FUS enters into a disease state (Figure 7): normally, FUS forms liquid compartments in cells. During transcription, FUS assembles into liquid compartments at active genes; during DNA damage, FUS assembles into liquid compartments at sites of DNA damage; under stress conditions, FUS rapidly shuttles to the cytoplasm and forms stress granules. The liquid nature of these compartments allows rapid diffusion necessary for chemical reactions on biological timescales. However, liquid formation comes with a cost: high local concentrations of a conformationally promiscuous protein. As cells age and the activity of the quality control machinery declines, and exacerbated by mutations that increase the aggregation propensities, FUS will convert into an aggregated state. Therefore, if a cell uses a dynamic liquid state to perform a physiological function, it will have to fight its whole life against the thermodynamic drive toward aggregate formation and disease.

We would like to reiterate that we do not think that fibrous aggregates represent the physiological function of FUS. Rather, the physiological function of the FUS protein is to act as a liquid, probably with little fixed structure. However, we currently have no information as to the molecular mechanism that drives the formation of a liquid-like state, apart from the fact that it requires the prion-like LC domain (Figure 7). The prion-like domain of FUS is intrinsically disordered, and the liquid state of FUS probably arises from its ability to sample many conformational states. Anything that increases the strength of interaction between prion-like domains could lead to formation of aggregates rather than liquids. Indeed, a mutant that we selected, G156E, maps to the prion-like domain and has been shown in vitro to exacerbate the aggregation potential of the protein (Nomura et al., 2014). This will presumably involve a number of conformational states, starting off with an increase in viscosity of the liquid and ending in the commonly seen aging-associated aggregates. Our EM data show that, in vitro, the liquid-like droplets are amorphous, without any obvious structure. Therefore, liquid formation itself does not require formation of obvious oligomers or fibers. However, it is possible, in vivo, that small oligomers are constantly forming and being disassembled by the quality control machinery. Future studies using cryo-EM will be required to investigate the structure of FUS compartments in vivo.

Our data do not address the issue of why aggregates are associated with disease. There are two possibilities: the aggregates themselves are toxic, or the proteins themselves, by being locked in a less dynamic state, are no longer able to perform their physiological function. In the case of FUS, this function is to help protect cells against stress, both in the nucleus and the cytoplasm. However, the intermediate biophysical states

discussed earlier could make cells more prone to stress, because the decrease in dynamics may impair the formation of stress compartments or the shuttling between the nucleus and the cytoplasm. It is possible that chemicals that slightly increase the fluidity of compartments could help ameliorate the development of the disease.

EXPERIMENTAL PROCEDURES

Detailed methods are available in the Supplemental Experimental Procedures.

Generation of Cell Lines

Stable HeLa cell lines expressing human FUS were generated using BAC recombineering technology (Poser et al., 2008).

DNA Damage Laser Cutting Assay

DNA damage was induced by applying 25 UV pulses at 12 equidistant dots along a 6-μm line within the nucleus using a laser micro-irradiation setup previously described (Behrndt et al., 2012; Mayer et al., 2010).

Stress and Inhibitor Treatment of HeLa Cells

The temperature increase from 37°C to 42°C, 1 mM sodium arsenate, or 720 Osm DMEM was used to induce heat, arsenate, or osmotic stress, respectively. The stress granules were imaged using a fast DSLM microscope with structured illumination (Planchon et al., 2011). We used 20 μg/ml of PARP inhibitor Abt-888 (Santa Cruz Biotechnology), 300 μM of PARG inhibitor Gallotannin (Santa Cruz Biotechnology), and 2.5 μg/ml of the transcription inhibitor actinomycin D (Sigma-Aldrich).

FUS Protein Purification from Insect Cells

Recombinant versions of FUS-GFP were purified using the baculovirus expression system (Hoell et al., 2011; Schwartz et al., 2012). Cells were lysed in resuspension buffer (50 mM Tris-HCl, 1 M KCl, 5% glycerol, 0.1% CHAPS, 1 mM DTT, pH 7.4), and FUS-GFP was captured using nickel-nitrilotriacetic acid (Ni-NTA) resin (QIAGEN) and eluted with elution buffer (resuspension buffer + 250 mM imidazole). His and MBP tags were cleaved off using a histidine-tagged Prescission Protease (in house) during dialysis against FUS dialysis buffer (50 mM Tris-HCl, 1 M KCl, 5% glycerol, 1 mM DTT, pH 7.4). Furthermore, size exclusion chromatography was performed with a Superdex 200 Increase 10/300 GL column (GE Healthcare Life Sciences) using an Akta Ettan fast protein liquid chromatography (FPLC) system (GE Healthcare Life Sciences).

Hydrogel Formation

MBP-FUS-GFP was concentrated to 500 μM (~50 mg/ml) in FUS dialysis buffer and dialyzed against FUS gelation buffer (20 mM Tris-HCl, 200 mM KCl, 0.5 mM EDTA, 1 mM DTT, pH 7.5) at 4°C for 48 hr to induce gelation (Kato et al., 2012).

In Vitro FUS Assays

FUS-GFP at indicated concentrations was incubated with 10% dextran (T500, Pharmacosmos) in 50 mM Tris-HCl, 500 mM KCl, 2.5% glycerol and 1 mM DTT, pH 7.4, for 10 min. To induce "aging," the assay was subjected to 12 rpm on a bench top rotator at room temperature.

SUPPLEMENTAL INFORMATION

Supplemental Information includes Supplemental Experimental Procedures, six figures, and seven movies and can be found with this article online at http://dx.doi.org/10.1016/j.cell.2015.07.047.

AUTHOR CONTRIBUTIONS

A. Patel and D.D. purified the FUS protein. A. Patel performed the in vitro experiments with FUS, with help from L.J, S.M., and H.O.L. H.O.L. performed the in vivo experiments with FUS, with help from S.M. and S. Stoynov. L.J., M.J., and S.G. performed and analyzed the in vitro fusion optical tweezer experiments. L.J. and S.M. analyzed the in vitro photobleaching experiments. S. Saha helped design the in vitro assay conditions. I.P. constructed all BAC cell lines. A. Pozniakovski constructed all clones. J.M. performed cryo-EM, with help from T.M.F. M.Y.H. performed mass spectrometry. N.M., L.A.R., M.W., and E.W.M. designed and built the DSLM. S.A. and A.A.H. conceived the project and wrote the paper, with help from A. Patel, H.O.L., and L.J.

ACKNOWLEDGMENTS

We thank the members of the S.A. and A.A.H. labs for helpful discussions; Barbara Borgonovo (Chromatography Facility) and Regis Lemaitre (Protein Expression and Purification Facility) for help with protein expression and purification; Benoit Lombardot for image analysis; Bert Nitzsche and Britta Schroth-Diez (Light Microscopy Facility) for help with light microscopy; and Annett Duemmler, Doris Richter, Marit Leuschner, and Andrea Ssykor for assistance with generating plasmids and BAC lines. We are grateful to Matthias Mann for support in determining the FUS concentration in HeLa cells and Wolfgang Baumeister for support with the cryo-EM experiments. We thank Suzanne Eaton, Andreas Hermann, Frank Jülicher, Timothy J. Mitchison, and Christopher A. Weber for helpful discussions and/or comments on the manuscript. We thank Jiri Lukas for sharing data before publication. We gratefully acknowledge funding from the Alexander von Humboldt Foundation (GRO/1156614 STP-2 to A. Patel, USA/1153678 STP to S. Saha, and INI/1155756 STP to S.M.), EMBO ALTF (608-2013 to S. Saha and 1131-2011 to J.M.), Human Frontier of Science (LT000685/2012-L to J.M.), the NSF of Bulgaria (DFNI-B02/16 to S. Stoynov), and the German Federal Ministry of Research and Education (BMBF 031A359A MaxSynBio to T.M.F. and 031A099 to N.M., L.R., M.W., and E.W.M.). This work is partly funded by the MaxSynBio consortium, which is jointly funded by the Federal Ministry of Education and Research of Germany and the Max Planck Society.

Received: January 22, 2015
Revised: May 10, 2015
Accepted: July 14, 2015
Published: August 27, 2015

REFERENCES

Aggarwal, S., Snaidero, N., Pähler, G., Frey, S., Sánchez, P., Zweckstetter, M., Janshoff, A., Schneider, A., Weil, M.T., Schaap, I.A., et al. (2013). Myelin membrane assembly is driven by a phase transition of myelin basic proteins into a cohesive protein meshwork. PLoS Biol. *11*, e1001577.

Alberti, S., Halfmann, R., King, O., Kapila, A., and Lindquist, S. (2009). A systematic survey identifies prions and illuminates sequence features of prionogenic proteins. Cell *137*, 146–158.

Banjade, S., and Rosen, M.K. (2014). Phase transitions of multivalent proteins can promote clustering of membrane receptors. eLife *3*, 3.

Behrndt, M., Salbreux, G., Campinho, P., Hauschild, R., Oswald, F., Roensch, J., Grill, S.W., and Heisenberg, C.P. (2012). Forces driving epithelial spreading in zebrafish gastrulation. Science *338*, 257–260.

Bosco, D.A., Lemay, N., Ko, H.K., Zhou, H., Burke, C., Kwiatkowski, T.J., Jr., Sapp, P., McKenna-Yasek, D., Brown, R.H., Jr., and Hayward, L.J. (2010). Mutant FUS proteins that cause amyotrophic lateral sclerosis incorporate into stress granules. Hum. Mol. Genet. *19*, 4160–4175.

Brangwynne, C.P., Eckmann, C.R., Courson, D.S., Rybarska, A., Hoege, C., Gharakhani, J., Julicher, F., and Hyman, A.A. (2009). Germline P granules are liquid droplets that localize by controlled dissolution/condensation. Science *324*, 1729–1732.

Brangwynne, C.P., Mitchison, T.J., and Hyman, A.A. (2011). Active liquid-like behavior of nucleoli determines their size and shape in Xenopus laevis oocytes. Proc. Natl. Acad. Sci. USA *108*, 4334–4339.

Decker, C.J., Teixeira, D., and Parker, R. (2007). Edc3p and a glutamine/asparagine-rich domain of Lsm4p function in processing body assembly in Saccharomyces cerevisiae. J. Cell Biol. *179*, 437–449.

Deng, H., Gao, K., and Jankovic, J. (2014). The role of FUS gene variants in neurodegenerative diseases. Nat. Rev. Neurol. *10*, 337–348.

Dumetz, A.C., Chockla, A.M., Kaler, E.W., and Lenhoff, A.M. (2008). Protein phase behavior in aqueous solutions: crystallization, liquid-liquid phase separation, gels, and aggregates. Biophys. J. *94*, 570–583.

Dutertre, M., Lambert, S., Carreira, A., Amor-Guéret, M., and Vagner, S. (2014). DNA damage: RNA-binding proteins protect from near and far. Trends Biochem. Sci. *39*, 141–149.

Galkin, O., and Vekilov, P.G. (2000). Control of protein crystal nucleation around the metastable liquid-liquid phase boundary. Proc. Natl. Acad. Sci. USA *97*, 6277–6281.

Galkin, O., Chen, K., Nagel, R.L., Hirsch, R.E., and Vekilov, P.G. (2002). Liquid-liquid separation in solutions of normal and sickle cell hemoglobin. Proc. Natl. Acad. Sci. USA *99*, 8479–8483.

Gao, L., Shao, L., Chen, B.C., and Betzig, E. (2014). 3D live fluorescence imaging of cellular dynamics using Bessel beam plane illumination microscopy. Nat. Protoc. *9*, 1083–1101.

Gilks, N., Kedersha, N., Ayodele, M., Shen, L., Stoecklin, G., Dember, L.M., and Anderson, P. (2004). Stress granule assembly is mediated by prion-like aggregation of TIA-1. Mol. Biol. Cell *15*, 5383–5398.

Gitler, A.D., and Shorter, J. (2011). RNA-binding proteins with prion-like domains in ALS and FTLD-U. Prion *5*, 179–187.

Han, T.W., Kato, M., Xie, S., Wu, L.C., Mirzaei, H., Pei, J., Chen, M., Xie, Y., Allen, J., Xiao, G., and McKnight, S.L. (2012). Cell-free formation of RNA granules: bound RNAs identify features and components of cellular assemblies. Cell *149*, 768–779.

Hoell, J.I., Larsson, E., Runge, S., Nusbaum, J.D., Duggimpudi, S., Farazi, T.A., Hafner, M., Borkhardt, A., Sander, C., and Tuschl, T. (2011). RNA targets of wild-type and mutant FET family proteins. Nat. Struct. Mol. Biol. *18*, 1428–1431.

Hubstenberger, A., Noble, S.L., Cameron, C., and Evans, T.C. (2013). Translation repressors, an RNA helicase, and developmental cues control RNP phase transitions during early development. Dev. Cell *27*, 161–173.

Hyman, A.A., and Brangwynne, C.P. (2011). Beyond stereospecificity: liquids and mesoscale organization of cytoplasm. Dev. Cell *21*, 14–16.

Hyman, A.A., Weber, C.A., and Jülicher, F. (2014). Liquid-liquid phase separation in biology. Annu. Rev. Cell Dev. Biol. *30*, 39–58.

Jucker, M., and Walker, L.C. (2013). Self-propagation of pathogenic protein aggregates in neurodegenerative diseases. Nature *501*, 45–51.

Kato, M., Han, T.W., Xie, S., Shi, K., Du, X., Wu, L.C., Mirzaei, H., Goldsmith, E.J., Longgood, J., Pei, J., et al. (2012). Cell-free formation of RNA granules: low complexity sequence domains form dynamic fibers within hydrogels. Cell *149*, 753–767.

Kedersha, N., Stoecklin, G., Ayodele, M., Yacono, P., Lykke-Andersen, J., Fritzler, M.J., Scheuner, D., Kaufman, R.J., Golan, D.E., and Anderson, P. (2005). Stress granules and processing bodies are dynamically linked sites of mRNP remodeling. J. Cell Biol. *169*, 871–884.

Kim, H.J., Kim, N.C., Wang, Y.D., Scarborough, E.A., Moore, J., Diaz, Z., MacLea, K.S., Freibaum, B., Li, S., Molliex, A., et al. (2013). Mutations in prion-like domains in hnRNPA2B1 and hnRNPA1 cause multisystem proteinopathy and ALS. Nature *495*, 467–473.

King, O.D., Gitler, A.D., and Shorter, J. (2012). The tip of the iceberg: RNA-binding proteins with prion-like domains in neurodegenerative disease. Brain Res. *1462*, 61–80.

Kwiatkowski, T.J., Jr., Bosco, D.A., Leclerc, A.L., Tamrazian, E., Vanderburg, C.R., Russ, C., Davis, A., Gilchrist, J., Kasarskis, E.J., Munsat, T., et al. (2009). Mutations in the FUS/TLS gene on chromosome 16 cause familial amyotrophic lateral sclerosis. Science *323*, 1205–1208.

Kwon, I., Kato, M., Xiang, S., Wu, L., Theodoropoulos, P., Mirzaei, H., Han, T., Xie, S., Corden, J.L., and McKnight, S.L. (2013). Phosphorylation-regulated binding of RNA polymerase II to fibrous polymers of low-complexity domains. Cell *155*, 1049–1060.

Kwon, I., Xiang, S., Kato, M., Wu, L., Theodoropoulos, P., Wang, T., Kim, J., Yun, J., Xie, Y., and McKnight, S.L. (2014). Poly-dipeptides encoded by the C9orf72 repeats bind nucleoli, impede RNA biogenesis, and kill cells. Science *345*, 1139–1145.

Lee, C.F., Brangwynne, C.P., Gharakhani, J., Hyman, A.A., and Jülicher, F. (2013). Spatial organization of the cell cytoplasm by position-dependent phase separation. Phys. Rev. Lett. *111*, 088101.

Li, P., Banjade, S., Cheng, H.C., Kim, S., Chen, B., Guo, L., Llaguno, M., Hollingsworth, J.V., King, D.S., Banani, S.F., et al. (2012). Phase transitions in the assembly of multivalent signalling proteins. Nature *483*, 336–340.

Li, Y.R., King, O.D., Shorter, J., and Gitler, A.D. (2013). Stress granules as crucibles of ALS pathogenesis. J. Cell Biol. *201*, 361–372.

Lomakin, A., Asherie, N., and Benedek, G.B. (2003). Liquid-solid transition in nuclei of protein crystals. Proc. Natl. Acad. Sci. USA *100*, 10254–10257.

Lukas, J., Lukas, C., and Bartek, J. (2011). More than just a focus: The chromatin response to DNA damage and its role in genome integrity maintenance. Nat. Cell Biol. *13*, 1161–1169.

Malinovska, L., Kroschwald, S., and Alberti, S. (2013). Protein disorder, prion propensities, and self-organizing macromolecular collectives. Biochim. Biophys. Acta *1834*, 918–931.

Mastrocola, A.S., Kim, S.H., Trinh, A.T., Rodenkirch, L.A., and Tibbetts, R.S. (2013). The RNA-binding protein fused in sarcoma (FUS) functions downstream of poly(ADP-ribose) polymerase (PARP) in response to DNA damage. J. Biol. Chem. *288*, 24731–24741.

Mayer, M., Depken, M., Bois, J.S., Jülicher, F., and Grill, S.W. (2010). Anisotropies in cortical tension reveal the physical basis of polarizing cortical flows. Nature *467*, 617–621.

Nomura, T., Watanabe, S., Kaneko, K., Yamanaka, K., Nukina, N., and Furukawa, Y. (2014). Intranuclear aggregation of mutant FUS/TLS as a molecular pathomechanism of amyotrophic lateral sclerosis. J. Biol. Chem. *289*, 1192–1202.

Planchon, T.A., Gao, L., Milkie, D.E., Davidson, M.W., Galbraith, J.A., Galbraith, C.G., and Betzig, E. (2011). Rapid three-dimensional isotropic imaging of living cells using Bessel beam plane illumination. Nat. Methods *8*, 417–423.

Polymenidou, M., Lagier-Tourenne, C., Hutt, K.R., Bennett, C.F., Cleveland, D.W., and Yeo, G.W. (2012). Misregulated RNA processing in amyotrophic lateral sclerosis. Brain Res. *1462*, 3–15.

Poser, I., Sarov, M., Hutchins, J.R., Hériché, J.K., Toyoda, Y., Pozniakovsky, A., Weigl, D., Nitzsche, A., Hegemann, B., Bird, A.W., et al. (2008). BAC TransgeneOmics: a high-throughput method for exploration of protein function in mammals. Nat. Methods *5*, 409–415.

Ramaswami, M., Taylor, J.P., and Parker, R. (2013). Altered ribostasis: RNA-protein granules in degenerative disorders. Cell *154*, 727–736.

Rulten, S.L., Rotheray, A., Green, R.L., Grundy, G.J., Moore, D.A., Gómez-Herreros, F., Hafezparast, M., and Caldecott, K.W. (2014). PARP-1 dependent recruitment of the amyotrophic lateral sclerosis-associated protein FUS/TLS to sites of oxidative DNA damage. Nucleic Acids Res. *42*, 307–314.

Schwartz, J.C., Ebmeier, C.C., Podell, E.R., Heimiller, J., Taatjes, D.J., and Cech, T.R. (2012). FUS binds the CTD of RNA polymerase II and regulates its phosphorylation at Ser2. Genes Dev. *26*, 2690–2695.

Serio, T.R., Cashikar, A.G., Kowal, A.S., Sawicki, G.J., Moslehi, J.J., Serpell, L., Arnsdorf, M.F., and Lindquist, S.L. (2000). Nucleated conformational conversion and the replication of conformational information by a prion determinant. Science *289*, 1317–1321.

Shelkovnikova, T.A., Robinson, H.K., Southcombe, J.A., Ninkina, N., and Buchman, V.L. (2014). Multistep process of FUS aggregation in the cell cytoplasm involves RNA-dependent and RNA-independent mechanisms. Hum. Mol. Genet. *23*, 5211–5226.

Strzelecka, M., Trowitzsch, S., Weber, G., Lührmann, R., Oates, A.C., and Neugebauer, K.M. (2010). Coilin-dependent snRNP assembly is essential for zebrafish embryogenesis. Nat. Struct. Mol. Biol. *17*, 403–409.

Sun, Z., Diaz, Z., Fang, X., Hart, M.P., Chesi, A., Shorter, J., and Gitler, A.D. (2011). Molecular determinants and genetic modifiers of aggregation and toxicity for the ALS disease protein FUS/TLS. PLoS Biol. *9*, e1000614.

Taylor, R.C., and Dillin, A. (2011). Aging as an event of proteostasis collapse. Cold Spring Harb. Perspect. Biol. *3*, a004440.

Toretsky, J.A., and Wright, P.E. (2014). Assemblages: functional units formed by cellular phase separation. J. Cell Biol. *206*, 579–588.

Vance, C., Rogelj, B., Hortobagyi, T., De Vos, K.J., Nishimura, A.L., Sreedharan, J., Hu, X., Smith, B., Ruddy, D., Wright, P., et al. (2009). Mutations in FUS, an RNA processing protein, cause familial amyotrophic lateral sclerosis type 6. Science *323*, 1208–1211.

Vekilov, P.G. (2004). Dense liquid precursor for the nucleation of ordered solid phases from solution. Cryst. Growth Des. *4*, 671–685.

Vekilov, P.G. (2010). Phase transitions of folded proteins. Soft Matter *6*, 5254–5272.

Wang, X., Arai, S., Song, X., Reichart, D., Du, K., Pascual, G., Tempst, P., Rosenfeld, M.G., Glass, C.K., and Kurokawa, R. (2008). Induced ncRNAs allosterically modify RNA-binding proteins in cis to inhibit transcription. Nature *454*, 126–130.

Wang, W.Y., Pan, L., Su, S.C., Quinn, E.J., Sasaki, M., Jimenez, J.C., Mackenzie, I.R., Huang, E.J., and Tsai, L.H. (2013). Interaction of FUS and HDAC1 regulates DNA damage response and repair in neurons. Nat. Neurosci. *16*, 1383–1391.

Weber, S.C., and Brangwynne, C.P. (2012). Getting RNA and protein in phase. Cell *149*, 1188–1191.

Wippich, F., Bodenmiller, B., Trajkovska, M.G., Wanka, S., Aebersold, R., and Pelkmans, L. (2013). Dual specificity kinase DYRK3 couples stress granule condensation/dissolution to mTORC1 signaling. Cell *152*, 791–805.

Wiśniewski, J.R., Hein, M.Y., Cox, J., and Mann, M. (2014). A "proteomic ruler" for protein copy number and concentration estimation without spike-in standards. Mol. Cell. Proteomics *13*, 3497–3506.

Woulfe, J., Gray, D.A., and Mackenzie, I.R. (2010). FUS-immunoreactive intranuclear inclusions in neurodegenerative disease. Brain Pathol. *20*, 589–597.

Yang, L., Gal, J., Chen, J., and Zhu, H. (2014). Self-assembled FUS binds active chromatin and regulates gene transcription. Proc. Natl. Acad. Sci. USA *111*, 17809–17814.